Hindawi
Advances in Materials Science and Engineering
Volume 2022, Article ID 8420785, 14 pages
https://doi.org/10.1155/2022/8420785

Research Article

Study of the Frost Resistance of HDFC Based on a Response Surface Model and GM (1,1) Model

Zeli Liu, Jiuhong Jiang, and Ziling Xu

School of Civil Engineering, Architecture and Environment, Hubei University of Technology, Wuhan 430068, China

Correspondence should be addressed to Jiuhong Jiang; 19910019@hbut.edu.cn

Received 16 November 2021; Accepted 14 December 2021; Published 21 January 2022

Academic Editor: V. Vijayan

Taking high ductility concrete (HDFC) as a research object, the frost resistance of HDFC in freeze-thaw cycle tests is studied, accurately predicted, and quantitatively described. Taking the relative dynamic elastic modulus as the evaluation index, the response surface model and GM (1,1) model were used to study the frost resistance of HDFC, and the advantages and disadvantages were evaluated. Design-Expert software was used to establish a response surface model to study the effects of polyvinyl alcohol fiber (PVA) length, polyvinyl alcohol fiber volume content, and number of freeze-thaw cycles on the frost resistance of HDFC, and a fitting relationship model between the relative dynamic elastic modulus and these three factors was established. The results show that the influence of PVA fiber content on the frost resistance durability of HDFC is higher than that of the PVA fiber length, but the effect of the external environment on the degree of deterioration for HDFC is greater than the improvement of the properties of the material itself; that is, the freeze-thaw cycling has a greater effect than the PVA fiber content and length. Grey system theory was introduced in the HDFC freezing resistance test, and the change rule for the relative elastic modulus and the average relative error for the GM (1,1) model for varying PVA fiber length and content was determined to be less than 5%. It is concluded that the freezing resistance prediction accuracy for HDFC based on the GM (1,1) model is higher than that of the response surface model. The GM (1,1) model can be used to accurately predict the degree of damage caused by freezing and melting cycles for HDFC.

1. Introduction

High ductility cement matrix composites are a new type of structural material with high toughness, high crack resistance, and high frost resistance. These materials show strong crack resistance and strain hardening under tensile and shear loads and can greatly improve the brittleness of concrete and have good prospects for development [1–6]. In the northern part of China, concrete structures are exposed to extremely harsh environments for extended periods of time, such as sand erosion, earthquake impact, sulfate erosion, and freeze-thaw damage. The loss of freeze-thaw damage is particularly serious, which affects the service life of structures and leads to great economic losses [7, 8]. Therefore, it is of great significance to study how to improve the frost resistance of concrete structures and evaluate the frost resistance of concrete structures for the reinforcement and maintenance of concrete structures under extreme weather conditions [9–13].

With the development of the concrete industry, concrete durability test methods based on various mathematical models continue to emerge, accelerating the development of civil construction industry. Based on response surface analysis, Wu et al. [14] concluded that freeze-thaw cycles and sulfate solution lead to the most significant damage to road concrete with high performance synthetic fiber in freeze-thaw cycle tests. Li Q et al. [15] established the response surface model for asphalt concrete fracture toughness and determined the relationship between the initial fracture toughness KQ and unstable fracture toughness KS. Based on the GM (1, 1) model, Gao et al. [16] established a frost resistance model of stress-damaged lightweight aggregate concrete under a special extreme environment and obtained high prediction accuracy. Kang et al. [17] established freeze-thaw

deterioration model for hydraulic concrete by using the grey residual GM (1,1) Markov model, which has high accuracy in the application calculation process. Based on fractal dimension theory and the GM (1,1) model, another research study [18] examined the macroscopic mechanics and microscopic pore structure of Aeolian sand lightweight aggregate concrete and established the grey GM (1,4) model for compressive strength.

Yang et al. [19] concluded the attenuation law for reinforced concrete structures in cold regions under the action of chloride salt and freeze-thaw cycles, and the concrete attenuation model obtained by nonlinear fitting can be used to predict the concrete life well. Yu et al. [20] studied the freeze-thaw cycle splitting test to simulate the frost heave characteristics of permeable asphalt concrete and used the Gray-Markov model to evaluate the groundwater stability in seasonal freeze-thaw areas, which has high accuracy. Riza Polat et al. [21] found that halloysite nanoclay, nano-CaO, and nano-SiO_2 are partial substitutes for cement to carry out mechanical properties and physical tests and found that 3% halloysite nanoclay has the highest durability and compressive strength. Dong et al. [11] studied the mechanical properties of concrete under the action of PE and steel fiber under freeze-thaw cycling. The results showed that the freeze-thaw cycle destroys the interfacial bonding of fibers, which is the main reason for deformation degradation. Li et al. [22] improved the durability of cement-based concrete under the combined action of freeze-thaw cycling and salt solution by reasonably adding AEA and multimineral content, optimizing the mix proportion of concrete by using a genetic algorithm. Finally, it was verified that the concrete has good durability under salt freezing. Kianoush Siamardi and Shahin Shabani [23] evaluated the freeze-thaw durability of short and long fibers for RCCP specimens, and the optimal ratio was obtained by fitting the regression model with the response surface method. Bin Chen and Jun Wang [24] studied the freeze-thaw damage amount and freeze-thaw damage model with sodium chlorate and sodium silicate as compound alkali activators. Cheng [25] studied the mechanical properties and durability of three types of high performance concrete (HPC). The tests showed that when the CFBC ash content is 20%, the compressive strength of HPC at the curing period of 28 d is the highest at 75 MPa and the strength loss after freeze-thaw cycling is the lowest of 0.17% and 0.81%.

On the one hand, few people have combined the response surface model with the GM (1,1) model to study the frost resistance model of HDFC, and the accuracy of these two models has not been compared. On the other hand, the response surface model is more suitable for discussing the correlation between the factors and the response in the experiment, and the GM (1,1) model is more suitable for data analysis with equal time intervals. In this work, a response surface model and GM (1,1) model were established to analyze and predict the frost resistance of HDFC with the number of freeze-thaw cycles, PVA volume content, and PVA length as variables. The simulation accuracy and pros and cons of the two models are discussed to provide a theoretical basis and experimental basis for solving the practical problems faced by cold areas in the north.

2. Experimental Phenomena

2.1. Mix Proportion and Test Scheme Design. According to the JGJ 55–2011 standard [26], HDFC mixes were designed. The concrete mix proportion design for the HDFC is presented in Table 1. Wuhan Huaxin cement P. O 42.5 R grade cement was adopted as the cementitious material; river sand was used as fine aggregate, fineness modulus of 1.85; the first grade fly ash specially used for scientific research in college was utilized as fly ash; natural gravel with good particle size distribution was used as the coarse aggregate, with a particle size of 5–20 mm; solid polycarboxylate superplasticizer was used to enhance the fluidity of HDFC, and the water reduction rate was 25%. High strength and high modulus polyvinyl alcohol fiber produced by Kuraray, Japan, was used; the mechanical properties of the fibers are shown in Table 2.

In this study, the fibers were soaked in mixing water to ensure complete distribution in the entire mixture and to prevent balling or tangling. The initial mixing procedure included cement and aggregate mixing for one minute, and then a water mixture with soaked fibers was added to the solid components and mixed thoroughly in a mixer for 5 minutes to achieve a homogeneous mixture. HDFC mixtures were cast in prismatic (100 × 100 × 400 mm) molds.

2.2. Experimental Methods. The rapid freeze-thaw method was tested according to the GB T50082-2009 standard [27]. The freeze-thaw cycles were soaked in water at 20–25°C for four days in advance and then placed into a rapid freeze-thaw machine for freeze-thaw cycle testing. The freeze-thaw cycle equipment utilized a the concrete rapid freeze-thaw testing machine produced by Hebei Tianjin Engineering Instrument, as shown in Figure 1(a). The mass loss rate is an important index to measure HDFC damage in freeze-thaw cycle tests. A high-precision quality detector was used to measure the test blocks after freeze-thaw cycles. The mass loss rate during the freeze-thaw cycle test was then determined. The relative dynamic elastic modulus of HDFC was measured, using a DT-18 concrete relative dynamic elastic modulus tester at the 25th, 50th, 75th, 100th, 125th, and 150th cycle. The relative dynamic elastic modulus tester is shown in Figure 1(b). The relative dynamic elastic modulus was calculated with

$$E_d = \frac{13.244 \times 10^{-4} \times WL^3 f^2}{a^4}, \quad (1)$$

where E_d is the modulus of dynamic elasticity of concrete before the freeze-thaw test (MPa), a is the edge length of the square cross-section test block, L is the edge length of the square cross-section test block, W is the mass of HDFC before the freeze-thaw test (kg), and f is the fundamental vibration frequency of the specimen under transverse vibration.

Table 1: Concrete mix proportion design of HDFC.

Code	Volume and length of PVA fiber		Dosage (kg/m^3)					
			Cement	Fly ash	Coarse aggregate	Fine aggregate	Water	Water-reducing agent
HDFC0-0	0	0	450	495	950	425	355	10
HDFC6-1	6	1.0%	450	495	950	425	355	10
HDFC6-1.5	6	1.5%	450	495	950	425	355	10
HDFC6-2	6	2.0%	450	495	950	425	355	10
HDFC9-1	9	1.0%	450	495	950	425	355	10
HDFC9-1.5	9	1.5%	450	495	950	425	355	10
HDFC9-2	9	2.0%	450	495	950	425	355	10
HDFC12-1	12	1.0%	450	495	950	425	355	10
HDFC12–1.5	12	1.5%	450	495	950	425	355	10
HDFC12.2	12	2.0%	450	495	950	425	355	10

Table 2: The performance index of PVA fiber.

Length (mm)	Diameter (μm)	Tensile strength (MPa)	Dynamic elastic modulus (GPa)	Elongation (%)	Density (g/cm^3)
6, 9, 12	39	1600	40	7	1.3

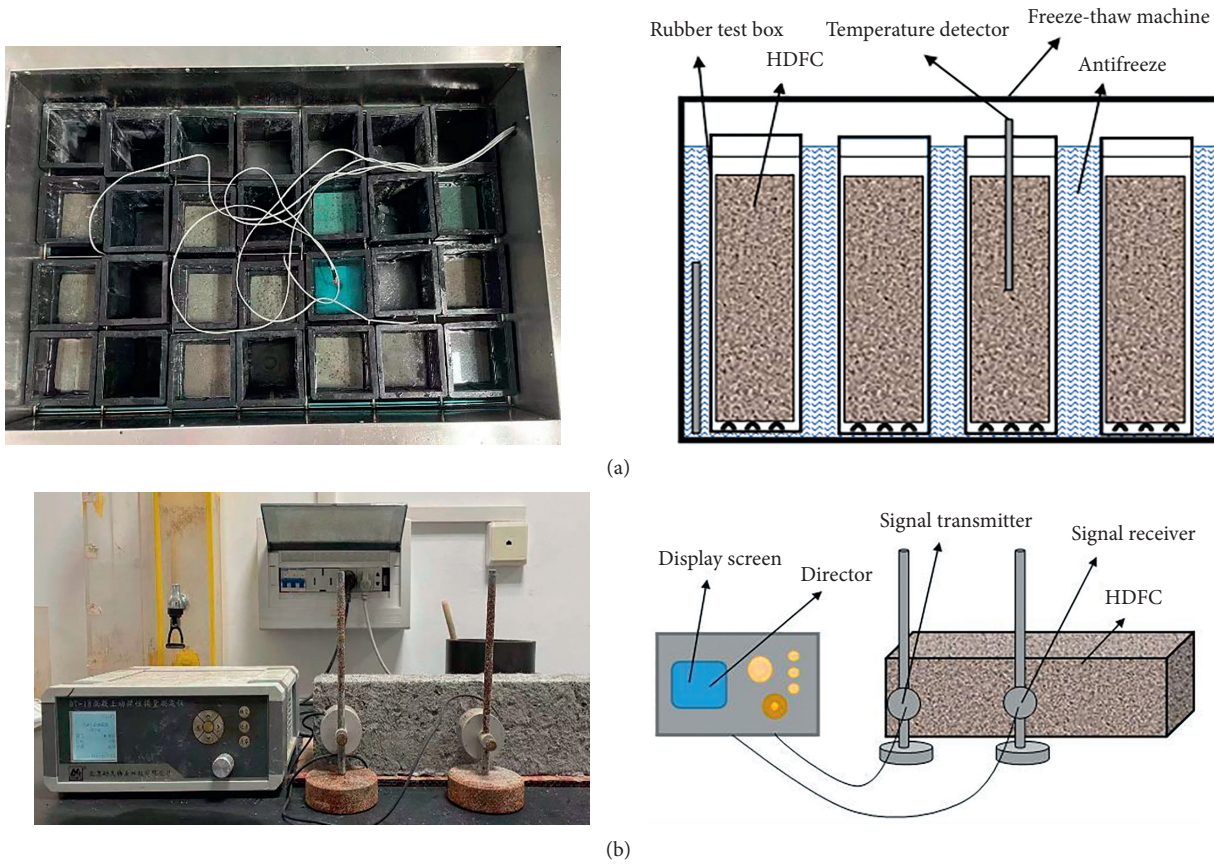

Figure 1: Test equipment diagram. (a) Freeze-thaw cycle machine. (b) Dynamic elastic modulus tester.

2.3. Relative Dynamic Elasticity of HDFC. In the freeze-thaw cycle test, the relative dynamic elastic modulus of each HDFC specimen varies with the number of freeze-thaw cycles as shown in Figure 2. Figure 2 shows that the relative dynamic elastic modulus of HDFC decreases with increasing number of freeze-thaw cycles. When the number of freeze-thaw cycles is 0–50, there is no obvious difference or observed dynamic modulus damage of the concrete and HDFC. A small amount of cementitious materials fell off the specimen surface. The relative dynamic elastic modulus

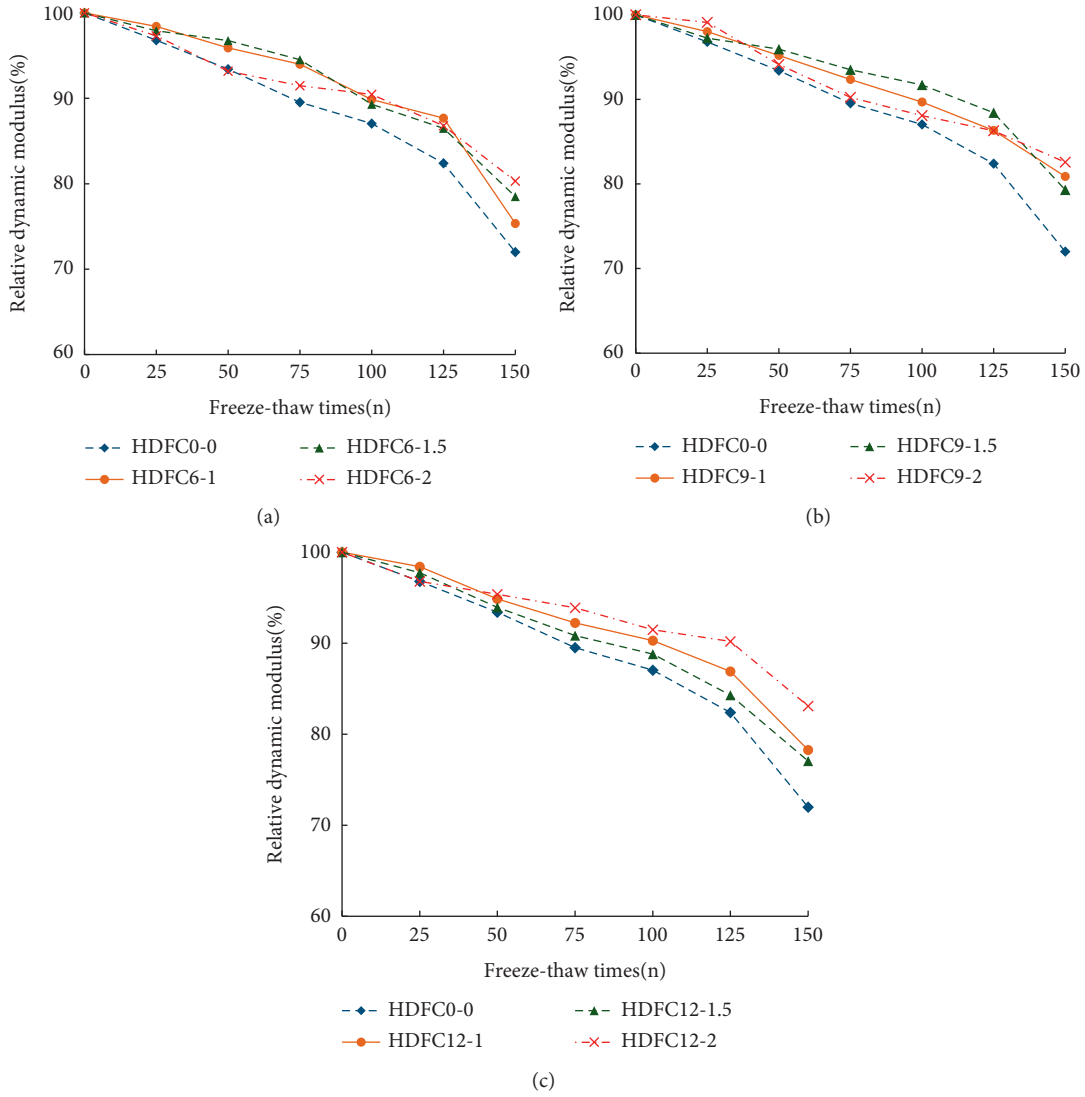

Figure 2: The change law of relative dynamic elastic modulus of HDFC. (a) HDFC6-1-HDFC6-2. (b) HDFC9-1-HDFC9-2. (c) HDFC12-1-HDFC12-2.

damage for the concrete is 8.5%; when the PVA content is 1.5% and the length is 9 mm, the minimum relative dynamic elastic modulus damage is 4.1%. When the number of freeze-thaw cycles reaches 50–100, the damage to the relative dynamic elastic modulus begins to become obvious, and more cementitious materials fall off the specimen surface. The relative dynamic elastic modulus damage for concrete is 13.9%; when the PVA content is 1.5% and the length is 9 mm, the minimum relative dynamic elastic modulus damage is 9.6%. When the number of freeze-thaw cycles reaches 100–150 times, the relative dynamic elastic modulus damage is the most serious, and much of the specimen surface falls off. The concrete begins to show a large number of fine cracks, and these cracks will accelerate the damage to the concrete due to the freeze-thaw cycling. However, the PVA fiber inside the concrete inhibits the development and extension of cracks, showing that the relative dynamic elastic modulus damage of HDFC is smaller than that of concrete. The relative dynamic elastic modulus damage for concrete is 28.1%, and the minimum relative dynamic elastic modulus damage is 17.9% when the PVA content is 2% and the length is 12 mm.

2.4. Mass Loss Rate for HDFC. In the process of freeze-thaw cycling, the quality loss for concrete is an important indicator to reflect the degree of freeze-thaw damage for concrete. The relationship between the mass loss rate and the number of freeze-thaw cycles was obtained through experiments, as shown in Figure 3. The mass loss rate for HDFC is far less than that for concrete. When the number of freeze-thaw cycles reaches 150, the mass loss rate for concrete does not reach 5%; that is, the concrete is not damaged. At the beginning of the freeze-thaw cycle, the quality of the concrete will increase slightly, and the quality growth will gradually decrease with the increasing of fiber content. When the PVA fiber content is 1.5%, the quality growth is the smallest. When the number of freeze-thaw cycles reaches

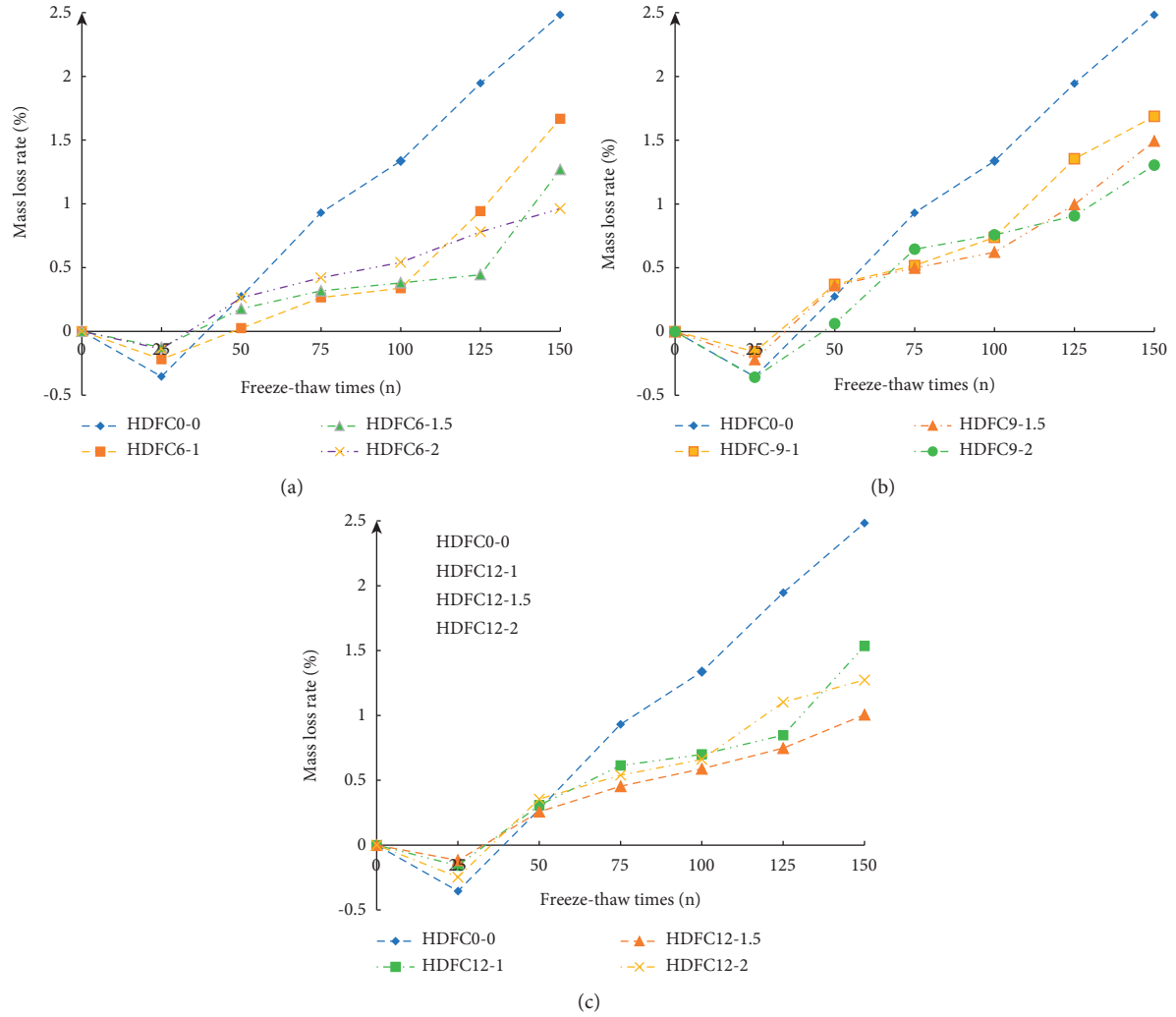

Figure 3: The relationship between mass loss rate and number of freeze-thaw cycles: (a) HDFC6-1-HDFC6-2. (b) HDFC9-1-HDFC9-2. (c) HDFC12-1-HDFC12-2.

50, the loss rate of the specimens begins to rise. Because the internal fiber in the specimen has the effect of an overarching connection, there will be no obvious cracks, and the overall performance remains good. With the freezing and thawing test, the internal crack damage for concrete will gradually drive the spalling of external aggregate and cementitious materials. The loss rate of the specimen is greater than the increase in internal pore water content, and the quality of the specimen begins to decrease. When the number of freeze-thaw cycles reaches more than 100, many internal fine cracks expanded into wide cracks and coarse aggregates begin to fall off, but the structure for HDFC is not loosened and still has a certain strength.

3. Frost Resistance of HDFC Based on Response Surface Methodology

3.1. Factor Level and Response. Response surface methodology (RSM) as a statistical method has been widely used in various industries. RSM can reflect the influence of each process variable on the target quantity in the experiment, can also reflect the interaction between multiple variables, and can include the combination of statistical mathematics technology. Finally, the relationship between variables and responses is reflected by a contour line map and three-dimensional images. However, RSM is rarely used in the study of the frost resistance durability of concrete.

PVA fibers significantly improve the frost resistance of concrete, in order to further study the influence of PVA fibers on the frost resistance of concrete. RS *M* was used to analyze the experimental results with the volume content of PVA as the A factor, the PVA length as the B factor, the number of freeze-thaw cycles as the C factor, and the relative dynamic elastic modulus as the *R* response. The factor coding and level are shown in Table 3. Design-Expert software was used to test and analyze the frost resistance of HDFC, and the quadratic response surface equation was selected to discuss the influence of three factors on the frost resistance of concrete, and the central design method was used to design the response surface method. The experimental results are shown in Table 4. The response surface equation considering all the

Table 3: Code and level of experimental factors.

Factor	Level		
	−1	0	1
PVA fiber content/A	1	1.5	2
Length of PVA fiber/B	6	9	12
Freeze-thaw times/C	50	100	150

Table 4: Experimental design and results.

Codes	Experimental design			Test result E_d (%)
	A (%)	B (mm)	C (times)	
1	1.5	6	150	78.49
2	1.5	12	150	77.04
3	1.0	12	100	90.31
4	2.0	12	100	91.47
5	1.0	9	50	95.19
6	2.0	9	50	94.12
7	1.5	6	50	96.57
8	1.5	12	50	93.95
9	2.0	9	150	82.57
10	1.0	9	150	80.87
11	1.5	9	100	91.71
12	1.5	9	100	90.35
13	2.0	6	100	90.46
14	1.5	9	100	91.1
15	1.0	6	100	93.88
16	1.5	9	100	89.55
17	1.5	9	100	91.11

coefficients of the first term, the second term, and the second cross term is given as follows:

$$R = \beta_0 + \sum_{i=1}^{k} \beta_i X_i + \sum_{i=1}^{k} \beta_{ii} X_i^2 + \sum_{i>j}^{k} \beta_{ij} X_i X_j + \varepsilon\left(X_i, X_j, \ldots, X_m\right), \tag{2}$$

where R is the response, X_i is a variable factor, $\beta_0, \beta_i, \beta_{ii}, \beta_{ij}$ are regression coefficients of the constant, primary, secondary, and cross terms, k is the number of variables, and ε represents the error (test error and fitting error).

3.2. Response Surface Model Establishment. Design-Expert software was now used for multivariate fitting analysis of the test data in Table 4, the regression model of the ternary single-phase surface (3). At the same time, the reliability, significance, and effectiveness of the model were analyzed. P and F values were used to express the validity and significance of the surface regression models. The pure error represents the degree of error between the fitted regression model and the experimental data. The coefficient of variation C.V was used to judge the reliability of the model. R^2 was used to judge the fitting effect.

$$R = 117.47 - 24.42A - 0.79B + 0.088C + 0.76AB + 0.028AC + 0.0023BC + 4.79A^2 - 0.048B^2 - 0.0015C^2, \tag{3}$$

where R is the response (relative dynamic elastic modulus), A is the content of PVA fiber content, B is the length of the PVA fiber, and C is the number of freeze-thaw cycles.

Variance analysis of the relative dynamic elastic modulus regression model for HDFC based on the response surface model is given in Table 5. The following conclusions can be drawn. The F value of the model is 28.29, and the output of the P value is 0.001 which is less than 0.05, indicating that the model has good effectiveness and reliability. The P value for the pure error is 0.0601 which is greater than 0.05, indicating that the error between the regression model and the experimental data is small and has a high correlation. The coefficient of variation C.V is 1.64%, and this value is less than 5%, indicating that the model has high reliability. The correlation coefficient $R^2 = 0.9732$, and the fitting degree and accuracy are very high. This indicates that this model can be well used to explain and predict the influence of the relative dynamic elastic modulus response under the interaction of PVA content, PVA length, and number of freeze-thaw cycles.

3.3. Analysis of the Model Results. The RSM scheme was imported into Design-Expert software, which can better predict the change relationship for R with the three factors and can be used to draw contour maps and three-dimensional response surface maps, as shown in Figures 4–6.

The analysis in Figure 4 shows that the change in the HDFC response R is not obviously affected by the A and B factors when the C factor is fixed. The performance along the length of the PVA fiber axis and PVA fiber content trend is relatively flat, but the trend of the A factor is slightly steeper than that of the B factor. Therefore, the effect of factor A on the HDFC response R is slightly greater than that of factor B. As shown by the contour map, A element and B factor contour densities are similar, which indicates that factors A and B have similar effects on the R response for HDFC.

From the three-dimensional response surface and contour map shown in Figure 5, it is obvious that the response R of HDFC is strongly influenced by the A and C factors. In the three-dimensional response surface diagram, the trend along factor C is significantly steeper than that along factor A. With the increasing of fiber content from 1% to 2%, the trend of the HDFC response R is first decreased and then increased, but the degree of change is not obvious. In the contour map, the density of the ordinate is higher than that of the abscissa. The contour map and response surface diagram also show that the external environment has a greater effect on the damage to HDFC than the material itself. That is to say, the influence of the C factor on the response R is greater than that of the A factor.

As shown by the analysis in Figure 6, the three-dimensional response surface curve shows that the response R for HDFC has a relatively steep trend along factor C and a relatively flat trend along factor B. In the contour map, the density of the ordinate is greater than that of the abscissa. Both images show that the influence of the C factor on the response R of HDFC is greater than that of the B factor. This shows that the external environment has a greater effect on

Table 5: Variance analysis of HDFC relative dynamic modulus regression model.

Source	Sum of squares	Df	Mean square	F value	P value
Model	545.09	9	60.57	28.29	0.0001
A	0.33	1	0.33	0.16	0.7054
B	5.80	1	5.80	2.71	0.1438
C	465.74	1	465.74	217.56	< 0.0001
AB	5.24	1	5.24	2.45	0.1615
AC	1.92	1	1.92	0.90	0.3754
BC	0.46	1	0.46	0.21	0.6585
A^2	6.04	1	6.04	2.82	0.1368
B^2	0.79	1	0.79	0.37	0.5637
C^2	59.99	1	59.99	28.02	0.0011
Residual	14.98	7	2.14	-	-
Pure error	2.77	3	4.07	5.87	0.0601

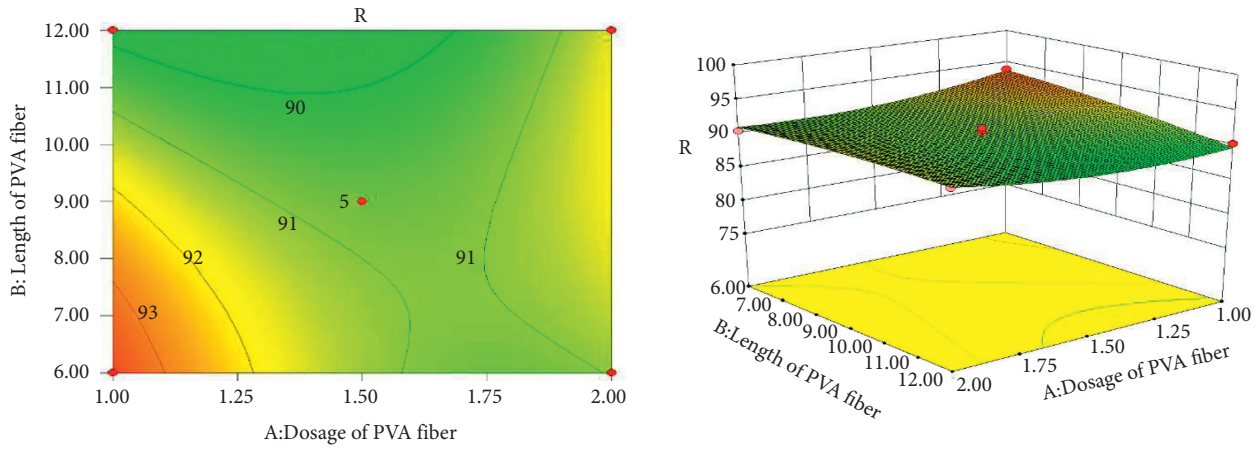

Figure 4: The effect of the interaction of A and B on R.

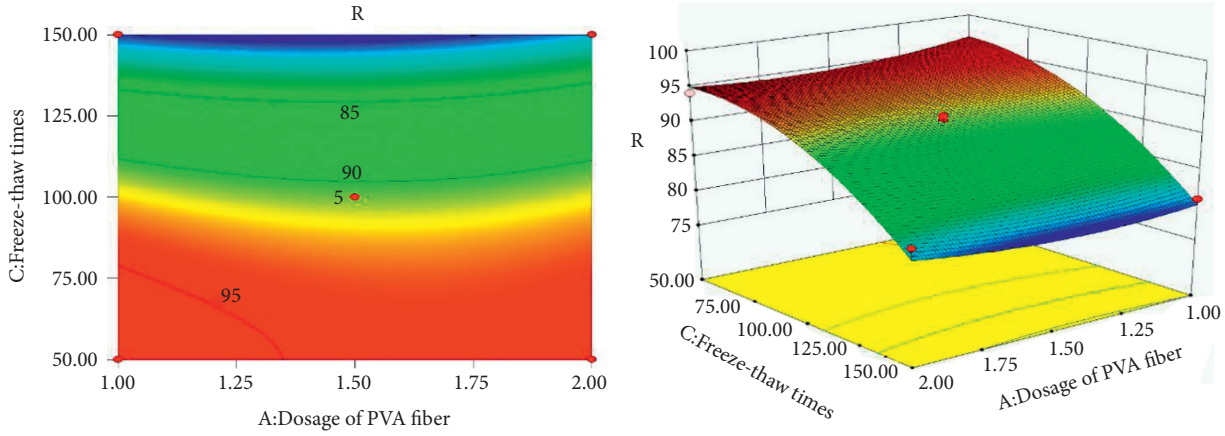

Figure 5: The effect of the interaction of A and C on R.

the degradation of HDFC than the material itself. In summary, the order of the significant degree of factor interaction is AC > BC > AB. Figures 7–9 show the residual normal distribution diagram, the distribution diagram for the predicted value and real values, and the distribution diagram for the residual and predicted values for the response surface model, respectively. It can be clearly observed that the residual normal distribution graph and the graph for the predicted and real values are basically distributed on both sides of a straight line. The distribution of data points in the distribution map of residual and predicted values is scattered and shows no obvious regularity. It can be concluded that the fitting data according to the response surface model conforms to the original law and the model has high accuracy in reflecting the change rule for the prediction response with three factors.

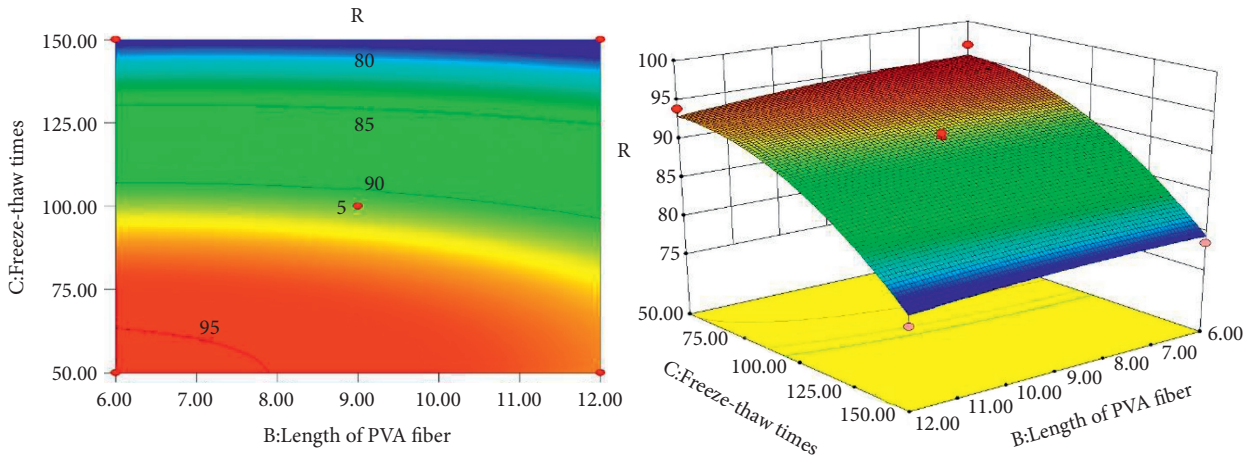

Figure 6: The effect of the interaction of B and C on R.

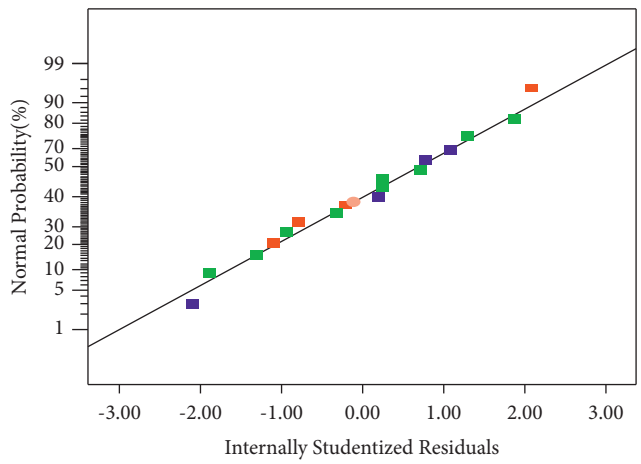

Figure 7: Residual distribution.

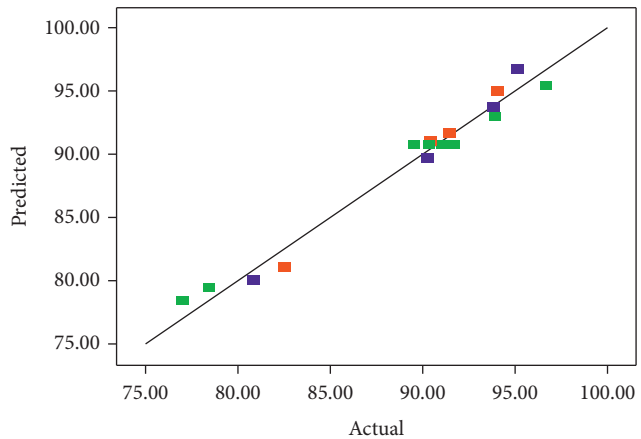

Figure 8: Predictions vs. actual values.

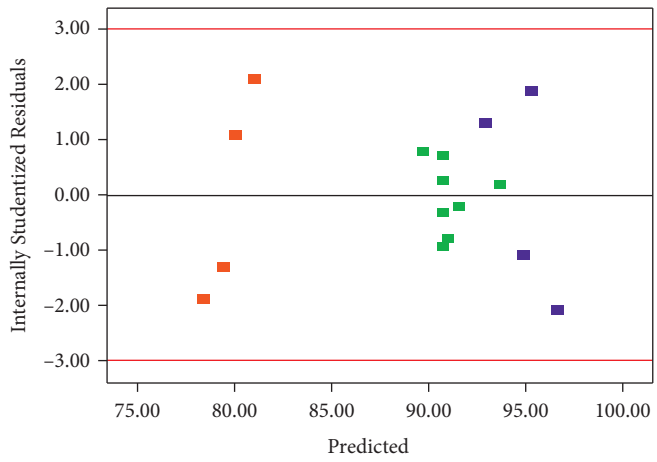

Figure 9: Residuals vs. predictions.

4. GM (1,1) HDFC Freeze-Thaw Damage Model

The GM (1,1) model is based on the initial sequence, first-order cumulative sequence, and background value [28]. The fitting curve was constructed by using the least squares method, and the albinism differential equation was established to solve the time response equation. The grey derivative information covering principle was used to solve the specific expression for the power functions. According to the minimum sequence for the average fitting relative error, the optimal weight was selected by automatic iteration to construct the background value, and the related properties of the power functions are discussed. The data sequence in the development prediction model with equal time intervals should be established. The GM (1,1) model requires that the data sequence changes gently and conforms to the nature of an exponential function and uses the residual correction model to correct the data to improve the prediction accuracy. Therefore, the GM (1,1) model is very suitable for processing and predicting the freeze-thaw cycle tests with equal time intervals.

4.1. GM (1,1) Model. The establishment process of the GM (1,1) model in this paper is to accumulate the relative dynamic elastic modulus loss of HDFC degradation to generate the a serial model. The freeze-thaw damage for HDFC can be predicted by serial processing. The original nonnegative data sequence is $X^{(0)}$:

$$X^{(0)} = \left(X_1^{(0)}, X_2^{(0)}, \ldots, X_n^{(0)}\right). \tag{4}$$

The first-order cumulative calculation of is $X^{(0)}$ conducted. Generating a first-order cumulative sequence 1 - AGO as $X^{(1)}$,

$$X_k^{(1)} = \sum_{i=1}^{k} X_1^{(0)} + X_2^{(0)} + \cdots + X_k^{(0)}, \quad k = 1, 2, \ldots, n, \tag{5}$$

$$X^{(1)} = \left(X_1^{(1)}, X_2^{(1)}, \ldots, X_n^{(1)}\right). \tag{6}$$

The sequence $Z^{(1)}$ adjacent to the mean value can be obtained by piecewise summation of (6). $Z^{(1)}$ is the background value of GM (1,1) model.

$$Z_k^{(1)} = 0.5\left(X_{k-1}^{(1)} + X_k^{(1)}\right), \quad k = 2, 3, \ldots, n, \tag{7}$$

$$Z^{(1)} = \left(Z_2^{(1)}, Z_3^{(1)}, \ldots, Z_n^{(1)}\right). \tag{8}$$

Next, albinism differential equation is established:

$$\frac{dX^{(1)}}{dt} + aX^{(1)} = b, \tag{9}$$

where the parameter a is the development coefficient, and the parameter b is the grey action. The least square method and MATLAB were used to determine the parameter values.

$$\hat{\alpha}[a, b]^T = \left[B^T B\right]^{-1} B^T Y, \tag{10}$$

$$Y = \begin{bmatrix} X_2^{(0)} \\ X_3^{(0)} \\ \vdots \\ X_n^{(0)} \end{bmatrix}, \quad B = \begin{bmatrix} -Z_2^{(1)} & 1 \\ -Z_3^{(1)} & 1 \\ \vdots & \vdots \\ -Z_n^{(1)} & 1 \end{bmatrix}. \tag{11}$$

The HDFC relative dynamic elastic modulus prediction model of the GM (1,1) model can be obtained by solving the albinism differential equation.

$$\widehat{X_k^{(1)}} = \left(X_1^{(0)} - \frac{b}{a}\right)e^{-a(k-1)} + \frac{b}{a}. \tag{12}$$

4.2. Relative Dynamic Elastic Modulus Prediction Model of GM (1,1). Based on the freeze-thaw tests, the first cumulative value (1-AGO) and background value of the relative

dynamic elastic modulus of HDFC are shown in Table 6. The HDFC relative dynamic elastic modulus prediction model and model parameters a and b for PVA fibers with different lengths and different dosages were calculated using formulas (4) – (12), as shown in Table 7.

5. Comparison and Error Analysis of the Models

5.1. Error Comparison between the GM (1,1) Model and Response Surface Model. Replace $k = 25$, 50, 75, 100, 125, and 150 with the relative dynamic elastic modulus prediction model in Table 7. By substituting the predicted results $\widehat{X_k^{(1)}}$ into the first-order cumulative calculation model, $\widehat{X_k^{(0)}}$ can be obtained. Based on the GM(1,1) model of different PV fiber lengths and contents under the influence of different freeze-thaw cycle times, the corresponding relative dynamic elastic modulus initial prediction value and relative error can be calculated as shown in Figure 9. Based on the response surface model research method, the fitting regression analysis for the relative dynamic elastic modulus for HDFC under the multifactor composite effect of PVA length, PVA content, and freeze-thaw cycles was considered to obtain the relationship between the various factors and response. The factors in (3) can be solved based on the response surface model for the HDFC relative dynamic elastic modulus prediction value and the relative error between the real values as shown in Figure 10.

Figure 10 shows that the relative error between the relative dynamic elastic modulus predicted by the GM (1,1) model with different PVA fiber contents and lengths is small. Moreover, the relative error does not change significantly with the increasing of freeze-thaw cycles, with a maximum average relative error of 4.3% and a minimum average relative error of 0.7%, and the average relative error is less than 5%. This indicates that the GM (1,1) model has high reliability for predicting the relative dynamic elastic modulus of HDFC to reflect the frost resistance of HDFC. The relative error of response surface model is generally higher than that of the GM (1,1) model. With the increasing number of freeze-thaw cycles, the relative error reflected by the response surface model will increase. The maximum average relative error of the response surface model is 6.2%, and the minimum average relative error is 5.4%; that is, the average relative error is greater than 5%. In summary, the overall accuracy of the GM (1,1) model for predicting the relative dynamic elastic modulus and frost resistance of HDFC is higher than that of the response surface model. Therefore, the GM (1,1) model has high reliability for the prediction of the relative dynamic elastic modulus and life cycle management of HDFC.

5.2. Accuracy Analysis of the GM (1,1) Model. To better analyze the prediction accuracy and reliability of the GM (1,1) model, the following indices can be used to analyze the prediction accuracy. The accuracy of the model is determined by the mean variance C, relative error a, and small error probability P. The static critical value of the established model is shown in Table 8. $\partial(k)$ is the residual of the original sequence $X^{(0)}$ and the prediction model $\widehat{X_k^{(1)}}$.

Relative error α :

$$\alpha = \left| \frac{X_k^{(1)} - \widehat{X_k^{(1)}}}{X_k^{(1)}} \right| \times 100\%. \tag{13}$$

Mean variance ratio C :

$$C = \frac{\sigma_2}{\sigma_1}, \tag{14}$$

where σ_1 is the mean variance of original data and σ_2 is the residual mean variance.

$$\sigma_1 = \frac{1}{n} \sum_{k=1}^{n} \left(X^{(0)} - \overline{X} \right), \tag{15}$$

$$\sigma_2 = \frac{1}{n} \sum_{k=1}^{n} \left(\partial(k) - \overline{\partial} \right). \tag{16}$$

Absolute correlation degree ε:

$$\varepsilon_{ij} = \frac{1 + |s_i| + |s_j|}{1 + |s_i| + |s_j| + |s_i - s_j|}, \tag{17}$$

$$|s_i| = \left| \sum_{k=2}^{n-1} X_k^{(0)} + \frac{1}{2} X_n^{(0)} \right|, \tag{18}$$

$$|s_j| = \left| \sum_{k=2}^{n-1} X_k^{(1)} + \frac{1}{2} X_n^{(1)} \right|, \tag{19}$$

$$|s_i - s_j| = \left| \sum_{k=2}^{n-1} \left(X_k^{(0)} - X_k^{(1)} \right) + \frac{1}{2} \left(X_n^{(0)} - X_n^{(1)} \right) \right|. \tag{20}$$

Probability of small error :

$$\partial(k) = X^{(0)} - \widehat{X_k^{(1)}}, \tag{21}$$

$$P = P\left\{ |\partial(k) - \overline{\partial}| < 0.6745\sigma_1 \right\}. \tag{22}$$

According to equations (13)–(22), the mean variance C, absolute correlation degree ε, relative error α, and small error probability P of the GM (1,1) model can be obtained. The results of C, ε, α, and P values calculated using the relative dynamic elastic modulus prediction model under the combined action of PVA fiber length and dosage are shown in Table 9. Table 9 shows that both the small error probability P and the mean square error ratio C of the HDFC relative dynamic elastic modulus prediction model are primary standards, which meet the accuracy prediction level of the GM (1,1) model. The average correlation degree ε of the model is higher than 0.9 at the primary standard, indicating that the model has high correlation. If the development coefficient a <0.3, the prediction of the relative dynamic elastic modulus in the GM (1,1) model is suitable for medium and long term prediction, and the prediction

Table 6: The background value of the relative dynamic elastic modulus of HDFC is 1-AGO.

Codes		Freeze-thaw times						
		0	25	50	75	100	125	150
HDFC0-0	Background value	—	148.3	243.5	334.9	423.2	508.0	585.2
	1-Ago	100	196.8	290	379.7	466.8	549.2	621.2
HDFC6-1	Background value	—	149.2	246.3	341.3	433.2	522.1	603.5
	1-Ago	100	198.4	294.3	388.3	478.2	565.8	641.2
HDFC6-1.5	Background value	—	149.0	246.3	341.9	433.9	521.8	604.3
	1-Ago	100	197.9	294.7	389.2	478.5	565.0	643.5
HDFC6-2	Background value	—	148.7	243.9	336.2	427.2	515.8	599.4
	1-Ago	100	197.3	290.5	381.9	472.4	559.2	639.6
HDFC9-1	Background value	—	149.0	245.6	339.4	430.4	518.4	639.5
	1-Ago	100	198.0	293.2	385.6	475.2	561.6	642.5
HDFC9-1.5	Background value	—	148.6	245.2	340.0	432.6	522.7	606.5
	1-Ago	100	197.2	293.2	386.7	478.4	566.9	646.2
HDFC9-2	Background value	—	149.6	246.2	338.3	427.5	514.7	599.1
	1-Ago	100	199.1	293.2	383.5	471.6	557.8	640.4
HDFC12-1	Background value	—	149.2	245.9	339.4	430.7	519.3	601.9
	1-Ago	100	198.4	293.3	385.5	475.8	562.7	641.0
HDFC12–1.5	Background value	—	148.9	244.7	337.1	426.9	513.5	594.2
	1-Ago	100	197.8	291.7	382.6	471.4	555.7	632.7
HDFC12.2	Background value	—	148.4	244.5	339.1	431.8	522.7	609.3
	1-Ago	100	196.8	292.2	386.1	477.6	567.8	650.8

Table 7: Prediction model and coefficient of relative dynamic elastic modulus of HDFC.

Codes	Parameters a and b	Relative dynamic elastic modulus prediction model
HDFC0-0	$a = 0.0516,\ b = 106.1338$	$\widehat{X_k^{(1)}} = -1956.86e^{-0.0516k} + 2056.86$
HDFC6-1	$a = 0.0447,\ b = 107.2912$	$\widehat{X_k^{(1)}} = -2300.25e^{-0.0447k} + 2400.25$
HDFC6-1.5	$a = 0.0415,\ b = 106.4648$	$\widehat{X_k^{(1)}} = -2465.42e^{-0.0415k} + 2565.42$
HDFC6-2	$a = 0.0331,\ b = 102.4197$	$\widehat{X_k^{(1)}} = -2994.25e^{-0.0331k} + 3094.25$
HDFC9-1	$a = 0.0343,\ b = 103.6657$	$\widehat{X_k^{(1)}} = -2922.32e^{-0.0343k} + 3022.32$
HDFC9-1.5	$a = 0.0352,\ b = 104.4933$	$\widehat{X_k^{(1)}} = -2868.56e^{-0.0352k} + 2968.56$
HDFC9-2	$a = 0.0345,\ b = 103.1350$	$\widehat{X_k^{(1)}} = -2889.42e^{-0.0345k} + 2989.42$
HDFC12-1	$a = 0.0395,\ b = 105.2368$	$\widehat{X_k^{(1)}} = -2564.22e^{-0.0395k} + 2664.22$
HDFC12–1.5	$a = 0.0430,\ b = 105.0253$	$\widehat{X_k^{(1)}} = -2342.45e^{-0.0430k} + 2442.45$
HDFC12–1.5	$a = 0.0284,\ b = 98.25320$	$\widehat{X_k^{(1)}} = -3359.62e^{-0.0284k} + 3459.62$

accuracy is high. The development coefficient a in the prediction model fitted by the GM (1,1) model is far less than 0.3, so the GM (1,1) model can be used to predict the freeze-thaw damage for HDFC over the whole life cycle [29].

6. Results and Discussion

(1) In a freeze-thaw cycle test, HDFC and concrete exhibit different degrees of deterioration, but HDFC shows better frost resistance than concrete. Regardless of the results of relative dynamic elastic modulus or the shedding of cementitious materials on the surface of concrete, HDFC is better than concrete. Under varying number of freeze-thaw cycles, the relative dynamic elastic modulus damage of HDFC is lower than that of ordinary concrete. When the PVA content is 2% and the length is 12 mm, the frost resistance of HDFC is the best.

(2) Through a response surface model established using Design-Expert software and the analysis of the residual error, real value, and predicted value image, in the process of freeze-thaw cycle testing, the influence of freeze-thaw cycles on the damage to the concrete is stronger than that of PVA fiber content and length, and the damage rate is greatly reduced with the addition of PVA fiber compared with concrete. However, the whole process of freeze-thaw damage remains unchanged; that is, the external environment has a greater effect on the degree of degradation

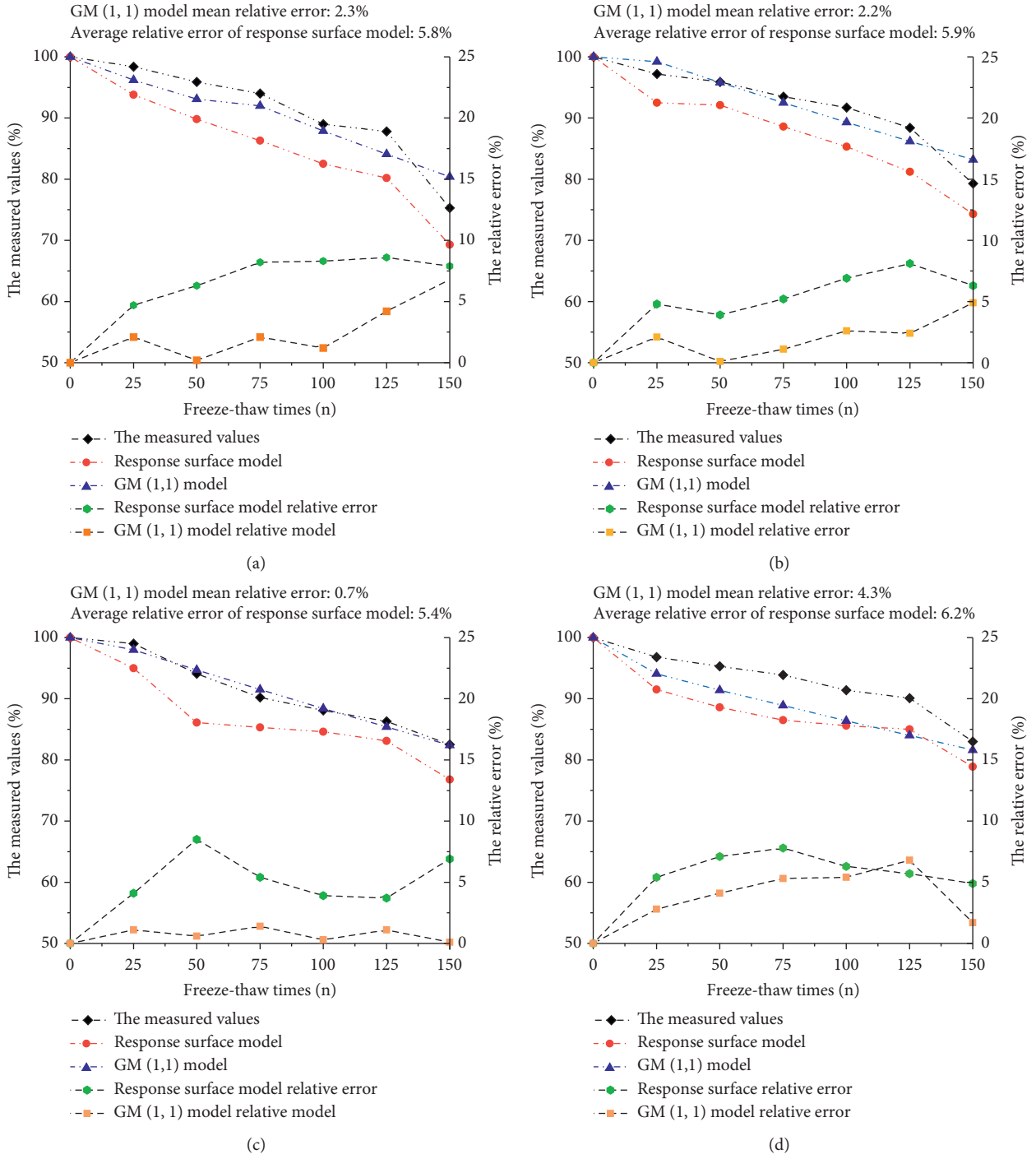

Figure 10: Accuracy comparison between GM (1,1) model and response surface model. (a) HDFC6-1. (b) HDFC9-1.5. (c) HDFC9-2. (d) HDFC12-2.

Table 8: Model established index critical value.

Critical value of the index	Accuracy class			
	Primary standard	Secondary standard	Three-level standard	Four-level standard
C	0.35	0.50	0.65	0.80
P	0.95	0.80	0.70	0.60
ε	0.90	0.80	0.70	0.60
α	0.01	0.05	0.10	0.20

Table 9: GM (1,1) model accuracy prediction table.

Critical value of the index	The relative dynamic elastic modulus prediction accuracy of GM (1,1) model									
	HDFC 0–0	HDFC 6–1	HDFC 6–1.5	HDFC 6–2	HDFC 9–1	HDFC 9–1.5	HDFC 9–2	HDFC 12–1	HDFC 12–1.5	HDFC 12–2
C	0.16	0.21	0.12	0.15	0.11	0.19	0.07	0.15	0.12	0.33
P	1.00	1.00	1.00	1.00	1.00	1.00	1.00	1.00	1.00	1.00
ε	0.9803	0.9731	0.9816	0.9763	0.9915	0.9756	0.9941	0.9833	0.9863	0.9658
α (%)	2.00	2.70	1.90	2.20	0.79	2.20	0.76	1.80	1.40	4.30

for HDFC than the material itself. It is concluded that the order of significance for the factor interaction is AC > BC > AB.

(3) By introducing the grey system theory, the average relative error in the relative dynamic elastic modulus prediction model fitted by the GM (1,1) model is less than 5%. Through comparative analysis, it can be found that the prediction accuracy of the GM (1,1) model for the relative dynamic elastic modulus of HDFC is higher than that of the response surface model. By analyzing the critical value of each index, the GM (1,1) model shows high prediction accuracy and reliability. This model can be used to predict the freeze-thaw damage for HDFC over the whole life cycle and provide a theoretical basis and experimental basis for the practical problems faced by the northern cold regions.

Data Availability

The data used to support the findings of this study are included within the article.

Conflicts of Interest

The authors declare that they have no conflicts of interest.

References

[1] V. C. Li and C. Leung, "Steady-state and multiple cracking of short random fiber composites," *Journal of Engineering Mechanics*, vol. 118, no. 11, 1992.

[2] V. C. Li, S. Wang, and C. Wu, "Tensile strain-hardening behavior of PVA-ECC," *ACI Materials Journal*, vol. 98, no. 6, pp. 483–492, 2011.

[3] V. C. Li, "Engineered cementitious composites–tailored composites through micromechanical modeling," *Journal of Advanced Concrete Technology*, vol. 1, p. 3, 1998.

[4] Q. Chunyu, C. Xu, S. Prannoy, W. W. Jason, and R. David, "Petrographic analysis of in-service cementitious mortar subject to freeze-thaw cycles and deicers," *Cement and Concrete Composites*, vol. 122, 2021.

[5] L. Yan, L. Xinping, and C. Andrew, "Damage constitutive model of single flaw sandstone under freeze-thaw and load," *Cold Regions Science and Technology*, vol. 159, pp. 20–28, 2019.

[6] W. Fang, N. Jiang, and X. Luo, "Establishment of damage statistical constitutive model of loaded rock and method for determining its parameters under freeze-thaw condition," *Cold Regions Science and Technology*, vol. 160, pp. 31–38, 2019.

[7] Y. Hong, Z. Kun, Z. Xiaoming, T. Zhizhuo, and Z. Qinglong, "Study on the freeze-thaw process of the lining structures of a tunnel on qinghai-tibet plateau with the consideration of lining frost damage," *Advances in Materials Science and Engineering*, vol. 2021, Article ID 4921365, 14 pages, 2021.

[8] S. Xian, Z. Lu, H. Yao, R. Fang, and J. She, "Comparative study on mechanical properties of compacted clay under freeze-thaw cycles with closed and open systems," *Advances in Materials Science and Engineering*, vol. 2019, Article ID 9206372, 13 pages, 2019.

[9] J. Tian, X. Wu, Y. Zheng, and S. Hu, "Investigation of damage behaviors of ECC-to-concrete interface and damage prediction model under salt freeze-thaw cycles," *Construction and Building Materials*, vol. 226, 2019.

[10] H. D. Yun, "Effect of accelerated freeze-thaw cycling on mechanical properties of hybrid PVA and PE fiber-reinforced strain-hardening cement-based composites (SHCCs)," *Composites Part B: Engineering*, vol. 52, 2013.

[11] F. Dong, H. Wang, J. Yu et al., "Effect of freeze-thaw cycling on mechanical properties of polyethylene fiber and steel fiber reinforced concrete," *Construction and Building Materials*, vol. 295, no. 4, Article ID 123427, 2021.

[12] F. Zhu, Z. Ma, and T. Zhao, "Influence of freeze-thaw damage on the steel corrosion and bond-slip behavior in the reinforced concrete," *Advances in Materials Science and Engineering*, vol. 2016, Article ID 9710678, 12 pages, 2016.

[13] Q. H. Xiao, Z. Y. Cao, X. Guan, Q. Li, and X. L. Liu, "Damage to recycled concrete with different aggregate substitution rates from the coupled action of freeze-thaw cycles and sulfate attack," *Construction and Building Materials*, vol. 221, pp. 74–83, 2019.

[14] Y. Wu, H. Wu, L. Cai, and W. Li, "Analysis of freeze - thaw and freeze - corrosion degradation of high-performance synthetic fiber pavement concrete based on response surface methodology," *Science and Technology*, vol. 20, no. 530, pp. 317–321, 2020.

[15] Q. Li, L. Cai, Y. Fu, H. Wang, and Y. Zou, "Fracture properties and response surface methodology model of alkali-slag concrete under freeze-thaw cycles," *Construction and Building Materials*, vol. 93, pp. 620–626, 2015.

[16] X. K. Gao and X. Shen, "Evaluation of frost resistance of stress-damaged lightweight aggregate concrete based on GM (1,1)," *Engineering Science and Technology*, vol. 53, no. 4, pp. 184–190, 2021.

[17] C. Kang, L. Gong, Z. Wang, T. Yang, and H. Wang, "Prediction of deterioration of hydraulic concrete by grey residual GM (1,1) -Markov model," *Journal of Water Conservancy and Water Transportation Engineering*, vol. 1, pp. 95–103, 2021.

[18] Q. Liu, X. Shen, L. Wei, R. Dong, and H. Xue, "Grey model research based on the pore structure fractal and strength of NMR aeolian sand lightweight Aggregate concrete," *Journal of the Minerals Metals & Materials Society*, vol. 72, no. 1, pp. 536–543, 2020.

[19] J. Yang, T. Zhang, and Q. Sun, "Experimental study on flexural fatigue properties of reinforced concrete beams after

salt freezing," *Advances in Materials Science and Engineering*, vol. 2020, Article ID 1032317, 15 pages, 2020.

[20] B. Yu, Z. Sun, and L. Qi, "Freeze-thaw splitting strength analysis of PAC based on the gray-markov model," *Advances in Materials Science and Engineering*, vol. 2021, Article ID 9954504, 12 pages, 2021.

[21] R. Polat, A. W. Qarluq, and F. Karagöl, "Influence of singular and binary nanomaterials on the physical, mechanical and durability properties of mortars subjected to elevated temperatures and freeze-thaw cycles," *Construction and Building Materials*, vol. 295, Article ID 123608, 2021.

[22] X. Li, W. Wang, Z. Zhu, and K. Zheng, "Investigation on durability behaviour and optimization of concrete with triple-admixtures subjected to freeze-thaw cycles in salt solution," *Advances in Materials Science and Engineering*, vol. 2021, Article ID 5572011, 16 pages, 2021.

[23] K. Siamardi and S. Shabani, "Evaluation the effect of micro-synthetic fiber on mechanical and freeze-thaw behavior of non-air-entrained roller compacted concrete pavement using response surface methodology," *Construction and Building Materials*, vol. 295, 2021.

[24] B. Chen and J. Wang, "Experimental study on the durability of alkali-activated slag. Concrete after freeze-thaw cycle," *Advances in Materials Science and Engineering*, vol. 2021, Article ID 9915639, 19 pages, 2021.

[25] Z. Cheng, L. He, L. Liu, Z. Cheng, X. Pei, and Z. Ma, "Mechanical properties and durability of high-performance concretes blended with circulating fluidized bed combustion ash and slag as replacement for ordinary portland cement," *Advances in Materials Science and Engineering*, vol. 2020, Article ID 8613106, 12 pages, 2020.

[26] China Buliding Materials Industry Press of the People's Republic of China, "Jgj 55-2011[S]: specification for design mix proportion of ordinary concrete," *Advances in Materials Science and Engineering*, China Buliding Materials Industry Press, Beijing, China, 2011.

[27] China Buliding Materials Industry Press of the People's Republic of China, "GB/T 50082-2009: standard for test methods of long-term performance and durability of ordinary concrete," *Advances in Materials Science and Engineering*, China Buliding Materials Industry Press, Beijing, China, 2009.

[28] S. F. Liu and J. L. Deng, "The range suitable for GM (1, 1)," *Systems Engineering-Theory & Practice*, vol. 11, pp. 131–138, 2000.

[29] Y. Hang and X. Xiao, "Difference analysis of morbidities of grey GM (1,1) derived model," *Systems engineering-theory & practice*, vol. 39, pp. 162–170, 2019.